Iranian Journal of Organic Chemistry Vol. 7, No. 4 (2015) 1631-1640

Density functional theory study of molecular structure, chemical reactivity and radical scavenging potency of (+)-curcutetraol

Mehdi Nabati*

Chemistry Department, Faculty of Science, Azarbaijan Shahid Madani University, Tabriz, Iran.

Received: September 2015; Revised: September 2015; Accepted: October 2015

Abstract: In the present work, I have studied the IR and NMR spectra, MEP plots, charge population analysis, Fukui indices and the antioxidant mechanisms of (+)-curcutetraol. All the calculations have been done by B3LYP/6-31G(d) level of theory in the gas phase at 298.15 K temperature and 1 atmosphere pressure. A comparison between the theoretical and experimental nuclear magnetic resonance (NMR) data indicates that the calculated results are consistent with the experimental values. And also, the similarity of the experimental and theoretical values of the bond lengths for compound shows the successful geometry optimization of the molecule at the used level of computations. The scavenging of hydroxyl, perhydroxyl, methylperoxy, superoxide, fluorine and nitroso radicals is carried out by sequential proton loss electron transfer (SPLET) mechanism, but the hydrogen atom transfer (HAT) mechanism is preferred to the scavenging of chlorine and bromine radicals.

Keywords: Curcutetraol, Antioxidant reactions, Fukui index, Free radical, DFT study.

Introduction

(+)-Curcutetraol was extracted from the marine fungus CNC-979 and bacterium CNH-741 by Lindel team in 2005. It is the first bisabolane sesquiterpenoid with a tertiary benzylic alcohol moiety as a single stereo-genic center in the O-position of a phenol isolated from the marine environment. The molecular structure of (+)-curcutetraol was determined on the basis of an extensive NMR spectroscopic analysis, and its absolute configuration was proposed to be *S* by the comparison of its experimental CD spectrum with the calculated one. To date, it is the most polar member of the phenolic bisabolane sesquiterpenoids with its four hydroxyl groups and it is the first bisabolane sesquiterpenoid with a tertiary benzylic alcohol moiety in the O-position of a phenol isolated from the marine environment. In 2008, Masatoshi Asami and his co-workers carried out the total synthesis of (+)-curcutetraol [1-6]. It strongly inhibits the activity of gastric H^+/K^+-ATPase. Gastric hydrogen/potassium-ATPase is an enzyme whose purpose is to acidify the stomach. It exchanges potassium from the intestinal lumen with cytoplasmic hydronium and is the enzyme primarily responsible for the acidification of the stomach contents and the activation of the digestive enzyme pepsin [7-9].

Computational chemistry (molecular modeling) is a beneficial tool that gives information about chemical and physical properties of materials without doing a physical experiment. It has been widely utilized in drug materials field [10-14]. A more precise approach has been established with the fast development in computer technology and theoretical chemistry. Computational chemistry facilitates the prediction of performances of drug molecules prior to the experimental work [14-18].

In this study, the main objectives of this work are (i) to perform a detailed calculation of the molecular

*Corresponding author. Tel: (+98) 413 4327501, Fax: (+98) 413 4327501, E-mail: mnabati@ymail.com

structure and chemical reactivity of (+)-curcutetraol and (ii) to investigate of influence of different free radicals on scavenging potency of (+)-curcutetraol.

Results and discussion

Structural properties

Scheme **1** shows the structure of (+)-curcutetraol with its labeling and atomic numbering. The geometry optimized structure of the compound computed at the B3LYP/6-31G(d) level of theory is presented in Figure **1**.

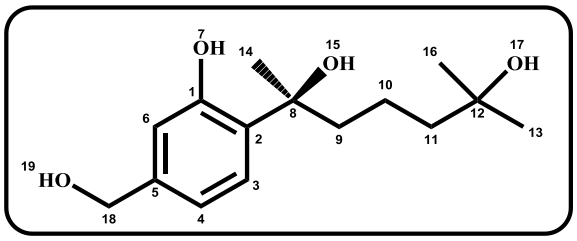

Scheme 1: Molecular structure of (+)-curcutetraol.

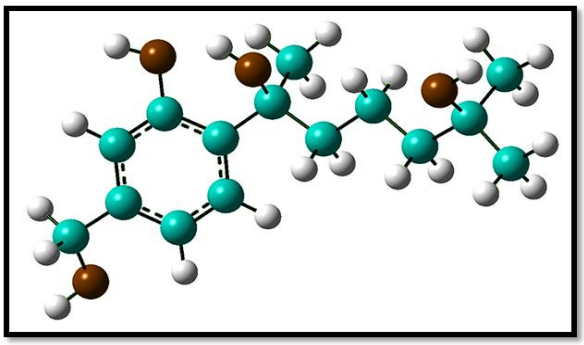

Figure 1: The geometry optimized (B3LYP/6-31G(d)) structure of present concern.

The bond lengths of the drug molecule calculated through mentioned level of theory are (Angstrom): 1.410 (C1-C2), 1.399 (C2-C3), 1.396 (C3-C4), 1.394 (C4-C5), 1.397 (C5-C6), 1.393 (C1-C6), 1.384 (C1-O7), 0.970 (O7-H7), 1.545 (C2-C8), 1.544 (C8-C9), 1.536 (C9-C10), 1.535 (C10-C11), 1.541 (C11-C12), 1.537 (C12-C13), 1.545 (C8-C14), 1.434 (C8-O15), 0.972 (O15-H15), 1.537 (C12-C16), 1.439 (C12-O17), 0.971 (O17-H17), 1.511 (C5-C18), 1.423 (C18-O19) and 0.969 (O19-H19).

Electrostatic potential maps, also known as electrostatic potential energy maps, or molecular electrical potential surfaces, illustrate the charge distributions of molecules three dimensionally. These maps allow us to visualize variably charged regions of a molecule [19, 20]. They also can be used to visualize the size and shape of molecules [21]. The 3-D electrostatic potential map of (+)-curcutetraol is shown in Figure **2**. The red loops and the blue loops indicate negative and positive charge development for a particular system respectively. As can be seen from the figure the negative charge is located on the oxygen elements as expected due to the electron withdrawing character of theirs and positive charge is located on the hydrogen atoms attached to the O7, O17 and O19 atoms.

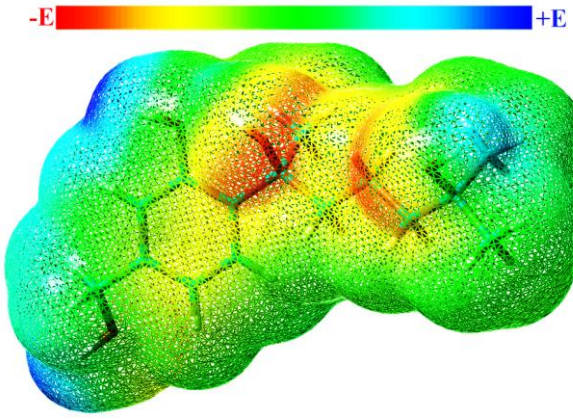

Figure 2: The 3-D electrostatic potential map of (+)-curcutetraol.

The Infra-Red (IR) spectrum is one basic property of a compound, and also an effective measure to identify structures [22, 23]. Figure **3** provides vibrational frequencies of (+)-curcutetraol.

Harmonic frequencies (cm^{-1}), IR intensities (KM/Mole): 30.9675 (0.3446), 39.7717 (1.6237), 42.0965 (0.3325), 54.9190 (2.7854), 79.9219 (1.2877), 82.2075 (1.6479), 128.1300 (0.0954), 134.3677 (1.6521), 148.4035 (1.4211), 189.6975 (1.0764), 197.0315 (3.1418), 225.0482 (2.9250), 238.2563 (1.1817), 252.3935 (0.3598), 272.1413 (0.5108), 279.1707 (0.1956), 286.4457 (0.0722), 310.2076 (5.0794), 334.0500 (5.6245), 340.9846 (78.0133), 345.7773 (12.8377), 372.5629 (56.2535), 374.4648 (4.7656), 379.9318 (21.4887), 386.7072 (133.8244), 397.4550 (14.0638), 419.6913 (5.3880), 424.0196 (7.2490), 462.2156 (16.7784), 481.3617 (2.9915), 517.8628 (4.0995), 523.0666 (15.5175), 543.0903 (122.7798), 556.0976 (4.1325), 578.3488 (12.6126), 594.5779 (12.3091), 645.3825 (3.7872), 710.1896 (4.6133), 742.0360 (4.0624), 756.0778 (6.5005), 758.8200 (7.2278), 777.3849 (8.9433), 835.7783 (36.9790), 841.9958 (0.5541), 847.7332 (0.6999), 872.5919 (7.8198), 920.3719 (1.5582), 933.6942 (0.5111), 953.5570 (29.6723), 960.4830 (25.1942), 966.2765 (0.1870), 976.4077 (5.4847), 997.1024 (8.7217), 1024.6753 (15.0128), 1034.7319 (3.9316), 1055.3800 (10.5370), 1062.3687 (6.0340), 1082.8071

(42.1850), 1093.9317 (58.3136), 1097.9363 (2.8392), 1149.1868 (15.7976), 1153.5784 (16.1010), 1170.8008 (63.6710), 1185.6166 (14.0659), 1196.2598 (6.2327), 1210.5270 (43.3313), 1214.7196 (103.5668), 1233.0049 (31.3367), 1242.0854 (96.0144), 1253.7677 (9.1674), 1265.2366 (23.4101), 1294.4483 (14.3991), 1299.7050 (1.8836), 1329.1087 (80.0495), 1334.3747 (0.9024), 1346.8707 (6.5018), 1361.4177 (24.0285), 1371.5614 (18.8970), 1391.6630 (28.9895), 1410.8047 (9.4566), 1413.0877 (43.6212), 1416.6204 (6.2627), 1425.2234 (110.7515), 1429.1801 (11.2289), 1449.0432 (49.7830), 1477.5926 (54.0934), 1486.4011 (1.1448), 1493.2748 (0.4776), 1499.2348 (0.5592), 1502.6785 (1.4859), 1510.6817 (1.3371), 1514.7139 (0.4898), 1521.4194 (1.1008), 1523.8889 (3.4362), 1525.7340 (9.9839), 1526.1228 (3.7351), 1559.9725 (2.8499), 1630.6894 (12.5850), 1675.5162 (27.2159), 2962.4494 (63.1119), 2990.0236 (58.3491), 3014.4478 (11.4467), 3020.6368 (14.7632), 3024.0309 (34.6921), 3028.5370 (36.2794), 3041.6690 (10.7987), 3047.2434 (12.4565), 3058.9288 (20.4321), 3071.3855 (44.9171), 3084.9501 (3.7953), 3092.7583 (68.1479), 3114.5988 (26.5920), 3115.8216 (22.9388), 3127.2913 (25.9801), 3128.3859 (34.5982), 3132.6596 (13.2029), 3136.3788 (22.7025), 3208.1013 (4.5753), 3223.5808 (6.5552), 3734.1234 (81.2680), 3752.6543 (4.9198), 3774.0627 (36.7255) and 3780.9897 (17.4717).

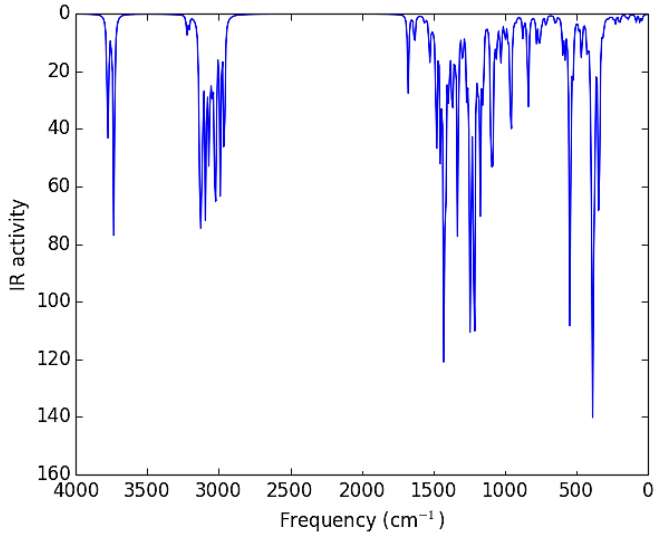

Figure 3: The IR spectrum of (+)-curcutetraol.

The calculation of nuclear magnetic resonance (NMR) parameters using density functional theory (DFT) techniques has become a major and powerful tool in the investigation to look at how variations in the molecular structure occurs. The ability to quickly evaluate and correlate the magnitude and orientation of the chemical shielding anisotropy tensor with variations in bond length, bond angles and local coordination and nearest neighbor interactions has been a number of recent applications in the investigation of molecular structure [24-26]. The calculated and experimental nucleus chemical shifts were reported in Table **1**. The dependence between theoretical and experimental chemical shifts data of (+)-curcutetraol is shown in Figure **4**. Higher correlation coefficient (R^2 = 0.9942) for them indicates a great convergence.

Table 1: Chemical shifts data of (+)-curcutetraol.

Nucleus	Chemical Shift (ppm)		
	Theoretical		Experimental
	δ'	δ = δ_{TMS} - δ'	δ (DMSO, 300MHz)
H-3	24.43	7.27	7.14
H-4	24.26	7.44	6.77
H-6	25.72	5.98	6.85
H-7	28.02	3.68	9.68
H-9	29.91	1.79	1.69
H-10	29.62	2.08	1.25
H-11	30.21	1.49	1.34
H-13	30.57	1.13	1.20
H-14	30.27	1.43	1.35
H-15	28.02	3.68	7.28
H-16	30.52	1.18	1.20
H-17	32.00	-0.30	4.49
H-18	27.42	4.28	4.61
H-19	31.53	0.17	5.27
C-1	44.44	147.06	158.9
C-2	59.14	132.36	128.7
C-3	69.21	122.29	129.7
C-4	77.24	114.26	119.5
C-5	56.62	134.88	139.8
C-6	85.19	106.31	114.4
C-8	116.61	74.89	70.1
C-9	149.15	42.35	45.4
C-10	171.20	20.30	11.5
C-11	147.87	43.63	44.3
C-12	120.89	70.61	72.3
C-13	157.72	33.78	29.8
C-14	164.38	27.12	29.7
C-16	163.05	28.45	29.8
C-18	126.42	65.08	65.0
O-7	224.64	-	-
O-15	270.87	-	-
O-17	249.97	-	-
O-19	306.08	-	-

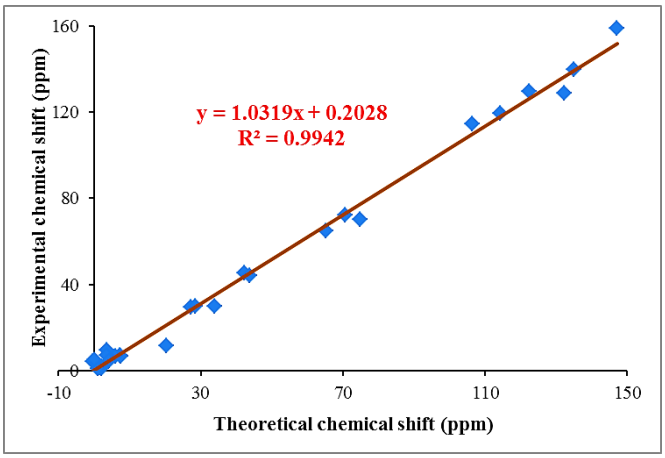

Figure 4: Correlation between calculated and experimental nucleus chemical shifts of (+)-curcutetraol at B3LYP level of theory with 6-31G(d) basis set.

Chemical reactivity:

Population analysis is the study of charge distribution within molecules [27]. The intention is to accurately model partial charge magnitude and location within a molecule. This can be thought of as a rigorous version of assigning partial charges on the atoms like chemists often do in Lewis dot structures [28]. Mulliken charges arise from the Mulliken population analysis and provide a means of estimating partial atomic charges from calculations carried out by the methods of computational chemistry, particularly those based on the linear combination of atomic orbitals molecular orbital method, and are routinely used as variables in linear regression (QSAR) procedures [29-31]. The method was developed by Robert S. Mulliken, after whom the method is named [32]. Figure **5** shows the Mulliken charge distribution on atoms of (+)-curcutetraol. We can see that the charge range within molecule is -0.591 to 0.591. The red loops and the green loops indicate negative and positive charge distribution for the atoms of the system respectively. The data of the charge distribution within the molecule indicates that the most negative and positive electronic charges are related to oxygen atoms and hydrogen atoms attached to the oxygen atoms, respectively.

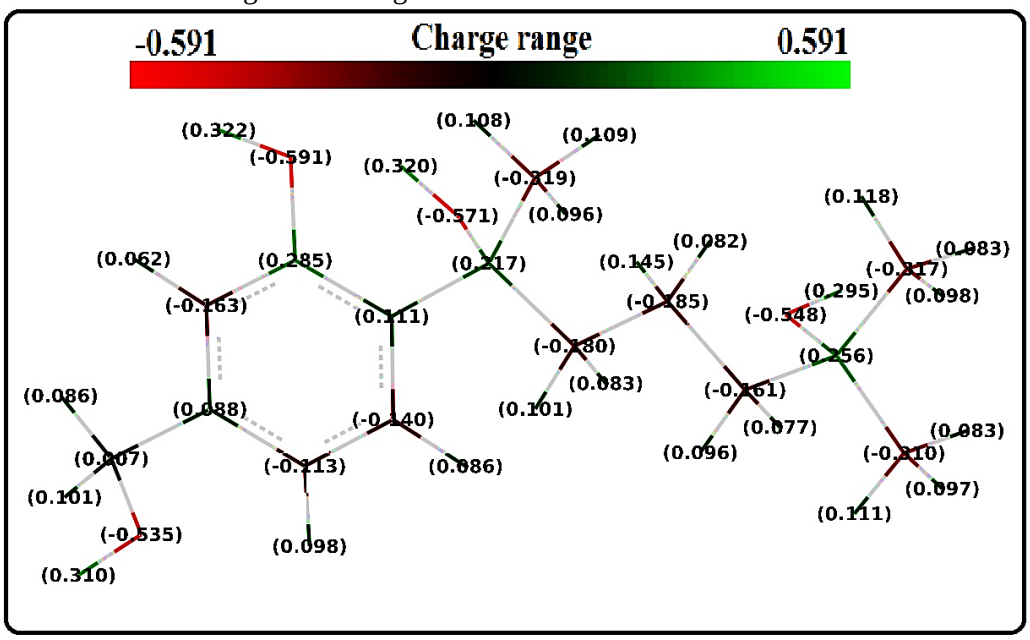

Figure 5: The Mulliken charge of atoms of (+)-curcutetraol.

In computational chemistry, the Fukui function or frontier function is a function that describes the electron density in a frontier orbital, as a result of a small change in the total number of electrons. The condensed Fukui function or condensed reactivity indicator is the same idea, but applied to an atom within a molecule, rather than a point in three-dimensional space [33]. The Fukui function allows one to predict, using density functional theory, where the most electrophilic and nucleophilic sites of a molecule are. The condensed Fukui functions were computed by taking the finite difference approximations from population analysis of atoms in molecules, depending on the direction of electron transfer, through the following formulas [34]:

$f_k^+ = q_{k(N+1)} - q_{k(N)}$ [for nucleophilic attack]

$f_k^- = q_{k(N)} - q_{k(N-1)}$ [for electrophilic attack]
$f_k^0 = [q_{k(N+1)} - q_{k(N-1)}]/2$ [for radical attack]
where q_k is the gross charge of atom k in the molecule.

Fukui indices indicate the reactive regions as well as the nucleophilic (the site for nucleophilic attack would depend on the values of f_k^+ on the atoms with a positive charge density), electrophilic (the sites for electrophilic attack will be those atoms bearing a negative charge and where the Fukui function f_k^- is a maximum) and radical attack (f_k^0) in the molecule [35]. Based on the data of Fukui indices of atoms in (+)-curcutetraol compound (Table **2**), the nucleophilic reactive order is: O7 > H4 > C1 > H6 > O15 > H3 > C4 > H18 > C2 > H7 > H14 > H19 > O17 > C6 > H9 = H17 > C3 = H16 > H13 > H15 > C18 > H10 = H11 > O19 = C5 > C13 > C9 = C16 > C11 > C10 > C12 > C14 > C8. The electrophilic order is: H4 > H19 > C2 > H3 > H18 > H6 > C18 > C6 > O15 > H14 > H7 > O7 > C1 > C3 > C4 > H9 = H10 > H15 = C8 > H17 = O19 > H13 > H11 > H16 > C16 > C5 > O17 > C12 > C10 = C13 > C11 > C9 > C14. The attack for free radicals is: H4 > H3 > H6 > C2 > O7 > H18 > H19 > O15 > C1 > C4 > H7 > C6 > H14 > C18 > C3 > H9 > H17 > H15 > H13 > O17 > H10 > H11 > H16 > O19 > C5 = C16 > C13 > C11 > C9 = C10 > C12 > C8 = C14.

Recently, second-order response of the electron density at the constant external potential *v(r)*, the Fukui function dual descriptor $f^{(2)}(r)$ defined by following equation, has been proposed for ambiphilic molecules and for reactions where there is a significant electron transfer or charge redistribution.

$$f^{(2)}(r) = \left(\frac{\partial^2 \rho(r)}{\partial N^2}\right)_{v(r)}$$

The Fukui function dual descriptor for a molecular system can be calculated by following equation or as a difference of the electron acceptor and the electron donor Fukui functions [36]:

$$f^{(2)}(r) = f^+(r) - f^-(r)$$

The negative and positive Fukui function dual descriptors are related to the favorable reactive sites for donating or accepting electron, respectively.

Table 2: Principal reactivity sites of (+)-curcutetraol molecule obtained by using Fukui indices.

Atom	Nucleophilic attack	Electrophilic attack	Radical attack	$f^{(2)}(r)$
H-3	0.064	0.081	0.072	-0.017
H-4	0.082	0.099	0.092	-0.017
H-6	0.069	0.073	0.071	-0.004
H-7	0.041	0.028	0.035	0.013
H-9	0.019, 0.023	0.013, 0.014	0.016, 0.019	0.008
H-10	0.003, 0.018	0.015, 0.012	0.009, 0.015	-0.003
H-11	0.012, 0.019	0.006, 0.008	0.009, 0.014	0.008
H-13	0.012, 0.017, 0.018	0.005, 0.007, 0.017	0.009, 0.012, 0.020	0.006
H-14	0.013, 0.043, 0.040	0.010, 0.056, 0.025	0.012, 0.050, 0.033	0.001
H-15	0.014	0.013	0.014	0.001
H-16	-0.003, 0.026, 0.017	-0.008, 0.020, 0.004	-0.006, 0.023, 0.011	0.008
H-17	0.021	0.010	0.016	0.011
H-18	0.049, 0.051	0.078, 0.071	0.065, 0.060	-0.025
H-19	0.031	0.093	0.062	-0.062
C-1	0.070	0.027	0.049	0.043
C-2	0.045	0.087	0.066	-0.042
C-3	0.020	0.024	0.022	-0.004
C-4	0.060	0.020	0.040	0.040
C-5	0.002	-0.001	-0.003	0.003
C-6	0.024	0.041	0.033	-0.017
C-8	-0.038	0.013	-0.026	-0.051
C-9	-0.005	-0.013	-0.009	0.008
C-10	-0.013	-0.005	-0.009	-0.008
C-11	-0.009	-0.007	-0.008	-0.002
C-12	-0.018	-0.003	-0.010	-0.015

C-13	-0.002	-0.005	-0.004	0.003
C-14	-0.031	-0.021	-0.026	-0.010
C-16	-0.005	0.000	-0.003	-0.005
C-18	0.012	0.047	0.030	-0.035
O-7	0.100	0.028	0.064	0.072
O-15	0.067	0.038	0.053	0.029
O-17	0.028	-0.002	0.013	0.030
O-19	0.002	0.010	0.007	-0.008

Influence of free radicals on scavenging potency of (+)-curcutetraol:

The O-H bonds homolytic cleavage in (+)-curcutetraol leads to the formation of four radicals. Figure **6** shows SOMOs and natural electron densities for all radicals. From the figures, only the unpaired electron of oxygen 7 (Rad-O7) can be delocalized.

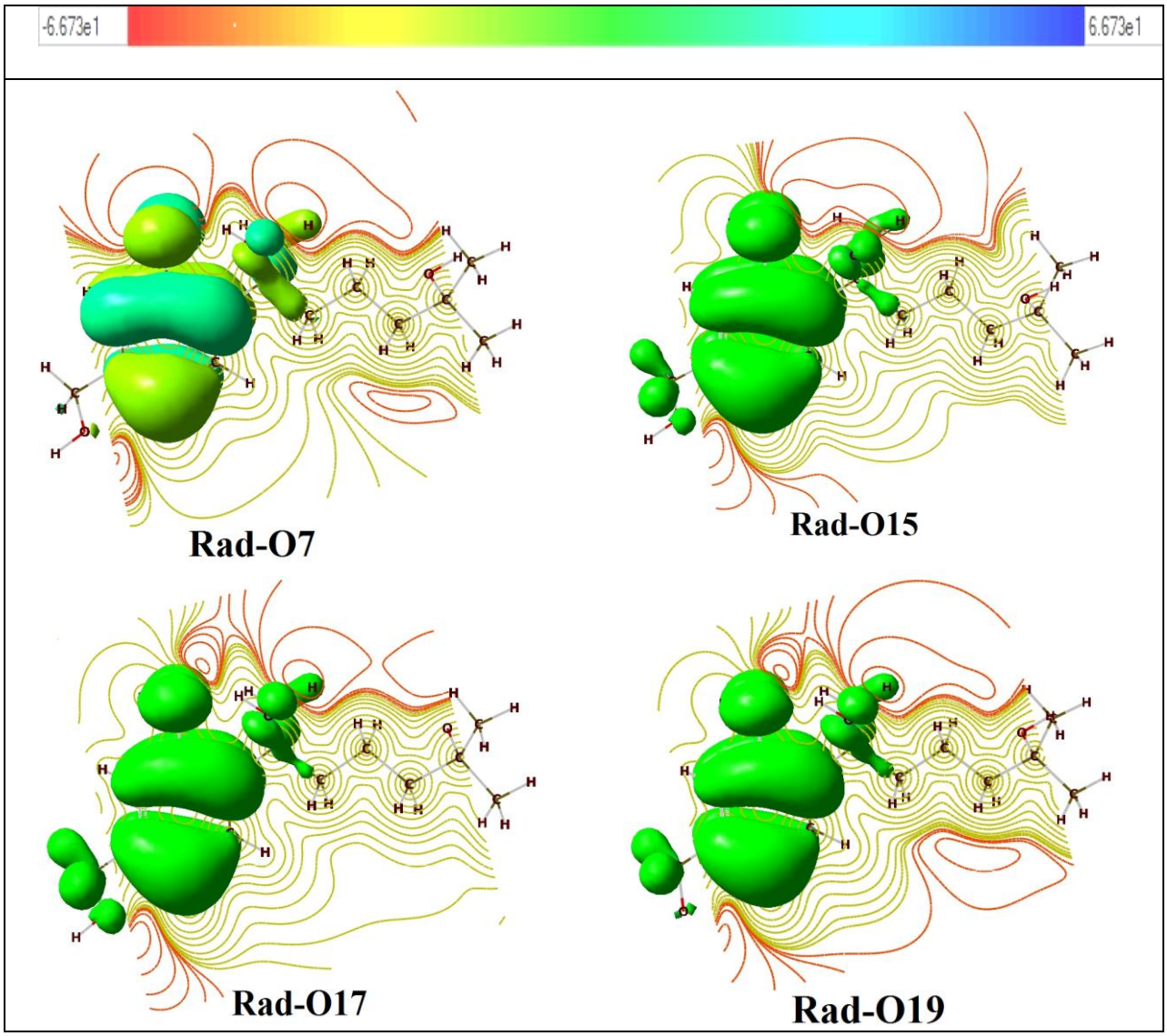

Figure 6: SOMOs of the (+)-curcutetraol molecule.

The abstraction of hydrogen atom from Ar-OH happens from three different mechanisms: hydrogen atom transfer (HAT), single electron transfer followed by proton transfer (SET-PT), and sequential proton loss electron transfer (SPLET) [37]. All three mechanisms with their enthalpies are listed in Table **3**.

Table 3: Three antioxidant mechanisms for (+)-curcutetraol molecule.

HAT	**ArOH → ArO$^{\cdot}$ + H$^{\cdot}$**	BDE = H(ArO$^{\cdot}$) + H(H$^{\cdot}$) – H(ArOH)
SET-PT	**ArOH → ArOH$^{\cdot+}$ + e$^-$**	IP = H(ArOH$^{\cdot+}$) + H(e$^-$) – H(ArOH)
	ArOH$^{\cdot+}$ → ArO$^{\cdot}$ + H$^+$	PDE = H(ArO$^{\cdot}$) + H(H$^+$) – H(ArOH$^{\cdot+}$)
SPLET	**ArOH → ArO$^-$ + H$^+$**	PA = H(ArO$^-$) + H(H$^+$) – H(ArOH)
	ArO$^-$ → ArO$^{\cdot}$ + e$^-$	ETE = H(ArO$^-$) + H(e$^-$) – H(ArO$^-$)

BDE: bond dissociation enthalpy, IP: ionization potential, PDE: proton dissociation enthalpy, PA: proton affinity, ETE: electron transfer enthalpy.

The energies of the antioxidant reactions for (+)-curcutetraol are calculated and shown in Table **4**. From the data, the bond dissociation enthalpy (BDE) value is lowest for the 7-OH functional group (323.8 kJ/mol). The unpaired electron of rad-O7 can be stabilized by resonance with pi electrons of benzene ring. And also, the order of relative BDE value for the oxygen radicals is: rad-O15 (73.167 kJ/mol) > rad-O17 (62.363 kJ/mol) > rad-O19 (47.138 kJ/mol) > rad-O7 (0.00 kJ/mol). The highest BDE value is related to the 15-OH group (397 kJ/mol). In single electron transfer followed by proton transfer (SET-PT) mechanism, the ionization potential (IP) energy for abstracting one electron from (+)-curcutetraol is 714.696 kJ/mol. The proton dissociation enthalpy (PDE) values suggest the transfer of proton is easier from the 7-OH group than from 15-OH, 17-OH and 19-OH groups. From the data, the lowest PDE value corresponds to the 7-OH group (874.556 kJ/mol). Akin to the two previous mechanisms of antioxidant reactions (BDE and SET-PT), the lowest proton affinity (PA) energy is for the 7-OH group (1385.902 kJ/mol). The relative PA energy order for hydroxyl groups of (+)-curcutetraol is: 17-OH (185.541 kJ/mol) > 15-OH (177.838 kJ/mol) > 19-OH (128.728 kJ/mol) > 7-OH (0.00 kJ/mol). And also, in second step of SPLET mechanism, the electron transfer enthalpy (ETE) order for OH groups is: 7-OH (203.351 kJ/mol) > 19-OH (148.016 kJ/mol) > 15-OH (124.935 kJ/mol) > 17-OH (106.428 kJ/mol). From the BDE, IP and PA values, the lowest enthalpy indicates the more favorable mechanism. Then, the hydrogen atom transfer (HAT) mechanism is thermodynamically more favorable.

Table 4: Calculated parameters of antioxidant mechanisms for (+)-curcutetraol molecule in kJ/mol.

Curcutetraol	HAT	SET-PT		SPLET	
	BDE	IP	PDE	PA	ETE
7-OH	323.777	714.696	874.556	1385.902	203.351
15-OH	396.944	714.696	973.979	1563.740	124.935
17-OH	386.140	714.696	963.175	1571.443	106.428
19-OH	370.915	714.696	947.950	1514.630	148.016

The scavenging mechanisms of various antioxidants are influenced by the properties of the scavenged radicals. The understanding of these properties can be obtained by enthalpy values of the antioxidant reactions. The exothermic and endothermic reactions are related to the favorable and unfavorable reaction paths, respectively [37]. Equations of the reaction of compound with different radicals are listed in Table **5**.

Table 5: The equations of (+)-curcutetraol molecule reaction with various radicals.

HAT	**ArOH + RO$^{\cdot}$ → ArO$^{\cdot}$ + ROH**	ΔH_{BDE} = H(ArO$^{\cdot}$) + H(ROH) – H(ArOH) – H(RO$^{\cdot}$)
SET-PT	**ArOH + RO$^{\cdot}$ → ArOH$^{\cdot+}$ + RO$^-$**	ΔH_{IP} = H(ArOH$^{\cdot+}$) + H(RO$^-$) – H(ArOH) – H(RO$^{\cdot}$)
	ArOH$^{\cdot+}$ + RO$^-$ → ArO$^{\cdot}$ + ROH	ΔH_{PDE} = H(ArO$^{\cdot}$) + H(ROH) – H(ArOH$^{\cdot+}$) – H(RO$^{\cdot}$)
SPLET	**ArOH + RO$^-$ → ArO$^-$ + ROH**	ΔH_{PA} = H(ArO$^-$) + H(ROH) – H(ArOH) - H(RO$^{\cdot}$)
	ArO$^-$ + RO$^{\cdot}$ → ArO$^{\cdot}$ + RO$^-$	ΔH_{ETE} = H(ArO$^{\cdot}$) + H(RO$^-$) – H(ArO$^-$) - H(RO$^{\cdot}$)

Table **6** indicates the reaction enthalpies of (+)-curcutetraol and eight radicals: hydroxyl radical, perhydroxyl radical, methylperoxy radical, superoxide radical anion, fluorine radical, chlorine radical, bromine radical and nitroso radical, related to the free radical scavenging activity mechanisms (HAT, SET-PT and SPLET) are calculated by density functional theory (DFT) method. In comparison of the BDE, IP and PA enthalpy values for the (+)-curcutetraol reaction with radicals, we can see the scavenging of hydroxyl, perhydroxyl, methylperoxy, superoxide, fluorine and nitroso radicals is performed by SPLET mechanism. And also, the HAT mechanism is

preferred to the scavenging of chlorine and bromine radicals. The proton affinity enthalpy order of hydroxyl (OH) groups of (+)-curcutetraol in scavenging of the hydroxyl, perhydroxyl, methylperoxy, fluorine and nitroso radicals is: 17-OH > 15-OH > 19-OH > 7-OH. It can be deduced that the 7-OH group of (+)-curcutetraol is more active in scavenging of mentioned radicals. Also, the PA order of OH groups in scavenging of superoxide anion radical is: 17-OH > 15-OH > 7-OH > 19-OH. It can be seen from the PA order; the 19-OH group is more active in scavenging of superoxide anion radical. The bond dissociation enthalpy (BDE) values of reaction of (+)-curcutetraol and chlorine and bromine radicals show the 15-OH > 17-OH > 19-OH > 7-OH order. We can see the active hydroxyl group of drug in scavenging of chlorine and bromine radicals is related to the 7-OH group.

Table 6: Calculated reaction enthalpies (kJ/mol) for the reaction of (+)-curcutetraol with different radicals.

Curcutetraol	HAT	SET-PT		SPLET	
	ΔH_{BDE}	ΔH_{IP}	ΔH_{PDE}	ΔH_{PA}	ΔH_{ETE}
CurOH-7 + rad-OH	-145.340	721.708	-867.048	-355.703	210.363
CurOH-7 + rad-HOO	-15.241	741.384	-756.625	-245.280	230.039
CurOH-7 + rad-CH_3OO	-10.272	704.079	-714.351	-203.008	192.732
CurOH-7 + rad-O_2^-	97.215	1694.403	-1597.183	-1085.840	1183.055
CurOH-7 + rad-F	-216.740	616.621	-833.365	-322.017	105.278
CurOH-7 + rad-Cl	-105.905	413.308	-519.213	-7.866	-98.039
CurOH-7 + rad-Br	-69.881	443.688	-513.565	-2.222	-67.659
CurOH-7 + rad-NO	120.524	916.430	-795.901	-284.558	405.082
CurOH-15 + rad-OH	-45.919	721.708	-767.626	-177.865	131.947
CurOH-15 + rad-HOO	84.181	741.384	-657.202	-67.441	151.623
CurOH-15 + rad-CH_3OO	89.149	704.079	-614.929	-25.168	114.317
CurOH-15 + rad-O_2^-	196.640	1694.403	-1497.762	-908.001	1104.641
CurOH-15 + rad-F	-117.318	616.621	-733.941	-144.179	26.862
CurOH-15 + rad-Cl	-6.482	413.308	-419.789	169.972	-176.455
CurOH-15 + rad-Br	29.542	443.688	-414.144	175.617	-146.075
CurOH-15 + rad-NO	219.949	916.430	-696.480	-106.719	326.668
CurOH-17 + rad-OH	-56.721	721.708	-778.430	-170.161	113.440
CurOH-17 + rad-HOO	73.378	741.384	-668.006	-59.738	133.116
CurOH-17 + rad-CH_3OO	78.345	704.079	-625.733	-17.465	95.810
CurOH-17 + rad-O_2^-	185.836	1694.403	-1508.566	-900.298	1086.133
CurOH-17 + rad-F	-128.122	616.621	-744.745	-136.476	8.354
CurOH-17 + rad-Cl	-17.286	413.308	-430.593	177.676	-194.962
CurOH-17 + rad-Br	18.738	443.688	-424.948	183.320	-164.582
CurOH-17 + rad-NO	209.145	916.430	-707.284	-99.016	308.160
CurOH-19 + rad-OH	-71.947	721.708	-793.655	-226.975	155.028
CurOH-19 + rad-HOO	58.152	741.384	-683.232	-116.551	174.704
CurOH-19 + rad-CH_3OO	63.120	704.079	-640.956	-74.275	137.398
CurOH-19 + rad-O_2^-	170.610	1694.403	-1523.791	-1425.947	1127.721
CurOH-19 + rad-F	-143.347	616.621	-759.970	-193.289	49.942
CurOH-19 + rad-Cl	-32.512	413.308	-445.818	120.862	-153.374
CurOH-19 + rad-Br	3.513	443.688	-440.173	126.507	-122.994
CurOH-19 + rad-NO	193.920	916.430	-722.509	-155.829	349.748

Conclusion

Presently, theoretical studies have been carried out on (+)-curcutetraol natural compound. The geometry of structure has been optimized at the theoretical level of B3LYP/6-31G(d). In the present work, the IR and NMR spectra, MEP plot, charge population analysis, Fukui indices and the antioxidant mechanisms of (+)-

curcutetraol have been determined and the following conclusions drawn:

(1) From the MEP plot, the negative charge is located on the oxygen elements as expected due to the electron withdrawing character of theirs and positive charge is located on the hydrogen atoms attached to the O7, O17 and O19 atoms.

(2) The oxygen atom that attached to the benzene ring is the favorable reactive site for accepting electron.

(3) The hydrogen atom transfer (HAT) mechanism is thermodynamically more favorable antioxidant mechanism.

(4) The scavenging of hydroxyl, perhydroxyl, methylperoxy, superoxide, fluorine and nitroso radicals is performed by SPLET mechanism.

(5) The HAT mechanism is preferred to the scavenging of chlorine and bromine radicals.

(6) The phenolic hydroxyl group is active hydroxyl group of the molecule in scavenging of radicals.

Computational method

All computations were done with the Gaussian 03 package [38] using the density functional theory (DFT) method. The calculations have been carried out by B3LYP/6-31G(d) level of theory. The exchange term of B3LYP contains hybrid Hartree-Fock (HF) and local spin density (LSD) exchange functions with Beck's gradient correlation to LSD exchange [39]. The correlation term of B3LYP consists of the Vosko, Wilk, Nusair (VWN3) local correlation functional [40] and the Lee, Yang, Parr (LYP) correlation correction functional [41, 42]. All the computations have been performed in the gas phase at 298.15 K temperature and 1 atm pressure.

Acknowledgement

Financial support from the Research Board of the Azarbaijan Shahid Madani University (ASMU) is gratefully acknowledged. I would also like to thank Doctor Mehrdad Mahkam for his valuable assistances.

References

[1] Mulhaupt, T.; Kaspar, H.; Otto, S.; Reichert, M.; Bringmann, G.; Lindel, T. *Eur. J. Org. Chem.* **2005,** *2005*, 334.

[2] Wagner-Dobler, I.; Beil, W.; Lang, S.; Meiners, M.; Laatsch, H. *Adv. Biochem. Eng. Sci.* **2002,** *74*, 207.

[3] Ito, S.; Zhang, C.; Hosoda, N.; Asami, M. *Tetrahedron* **2008,** *64*, 9879.

[4] Serra, S.; Cominetti, A. A. *Tetrahedron: Asymmetry* **2013,** *24*, 1110.

[5] Zhang, C.; Ito, S.; Hosoda, N.; Asami, M. *Tetrahedron Lett.* **2008,** *49*, 2552.

[6] Kudo, S.; Murakami, T.; Miyanishi, J.; Tanaka, K.; Takada, N.; Hashimoto, M. *Biosci. Biotechnol. Biochem.* **2009,** *73*, 203.

[7] Fujii, T.; Takahashi, Y.; Takeshima, H.; Saitoh, C.; Shimizu, T.; Takeguchi, N.; Sakai, H. *Eur. J. Pharmacol.* **2015,** *765*, 34.

[8] Schatzberg, D.; Lawton, M.; Hadyniak, S. E.; Ross, E. J.; Carney, T.; Beane, W. S.; Levin, M.; Bradham, C. A. *Dev. Biol.* **2015,** *406*, 259.

[9] Scott, D. R.; Munson, K. B.; Marcus, E. A.; Lambrecht, N. W. G.; Sachs, G. *Aliment. Pharm. Ther.* **2015,** *42*, 1315.

[10] Mahkam, M.; Nabati, M.; Latifpour, A.; Aboudi, J. *Des. Monomers Polym.* **2014,** *17*, 453.

[11] Mahkam, M.; Namazifar, Z.; Nabati, M.; Aboudi, J. *Iran. J. Org. Chem.* **2014,** *6*, 1217.

[12] Nabati, M.; Mahkam, M. *Iran. Chem. Commun.* **2014,** *2*, 164.

[13] Nabati, M.; Mahkam, M.; Heidari, H. *Iran. Chem. Commun.* **2014,** *2*, 236.

[14] Nabati, M.; Mahkam, M. *Iran. J. Org. Chem.* **2013,** *5*, 1157.

[15] Nabati, M.; Mahkam, M. *Iran. Chem. Commun.*, **2014,** *2*, 129.

[16] Mahkam, M.; Nabati, M.; Kafshboran, H. R. *Iran. Chem. Commun.* **2014,** *2*, 34.

[17] Mahkam, M.; Kafshboran, H. R.; Nabati, M. *Des. Monomers Polym.* **2014,** *17*, 784.

[18] Teymori, A.; Amiri, S.; Massoumi, B.; Mahkam, M.; Nabati, M. *Iran. J. Org. Chem.* **2014,** *6*, 1287.

[19] Nabati, M.; Mahkam, M. *Iran. J. Org. Chem.* **2015,** *7*, 1537.

[20] Nabati, M.; Mahkam, M. *Iran. J. Org. Chem.* **2015,** *7*, 1419.

[21] Nabati, M.; Mahkam, M. *Iran. J. Org. Chem.* **2015,** *7*, 1503.

[22] Nabati, M.; Mahkam, M. *J. Phys. Theor. Chem. IAU Iran* **2015,** *12*, 121.

[23] Nabati, M.; Mahkam, M. *Iran. J. Org. Chem.* **2014,** *6*, 1397.

[24] Nabati, M.; Mahkam, M. *Iran. J. Org. Chem.* **2014,** *6*, 1331.

[25] Aboudi, J.; Bayat, Y.; Abedi, Y.; Nabati, M.; Mahkam, M. *Iran. J. Chem. Chem. Eng.* **2015,** *34*, 1.

[26] Nabati, M.; Mahkam, M. *Iran. J. Org. Chem.* **2015,** *7*, 1463.

[27] Nabati, M.; Mahkam, M. *J. Phys. Theor. Chem. IAU Iran* **2015,** *12*, 33.

[28] La Pierre, H. S.; Rosenzweig, M.; Kosog, B.; Hauser, C.; Heinemann, F. W.; Liddle, S. T.; Meyer, K. *Chem. Commun.* **2015,** *51*, 16671.

[29] He, C.; Huang, R. Y.; Shi, Z. Q.; Zhang, W. X. *Mater. Tech.* **2015,** *30*, A36.

[30] Bauza, A.; Frontera, A.; Mooibroek, T. J.; Reedijk, J. *CrystEngComm* **2015,** *17,* 3768.
[31] Li, C.; Fan, B.; Li, W.; Wen, L.; Liu, Y.; Wang, T.; Sheng, K.; Yin, Y. *J. Korean Phys. Soc.* **2015,** *66,* 1789.
[32] Azimi, A.; Javanbakht, M. *Anal. Chim. Acta* **2014,** *812,* 184.
[33] Bhattacharjee, R. Roy, R. K. *Phys. Chem. Chem. Phys.* **2014,** *16,* 22237.
[34] Sagdinc, S.; Kara, Y.; Kayadibi, F. *Can. J. Chem.* **2014,** *92,* 876.
[35] Vargas-Sanchez, R. D.; Mendoza-Wilson, A. M.; Balandran-Quintana, R. R.; Torrescano-Urrutia, G. R.; Sanchez-Escalante, A. *Comp. Theor. Chem.* **2015,** *1058,* 21.
[36] Beker, W.; Stachowicz-Kusnierz, A.; Zaklika, J.; Ziobro, A.; Ordon, P.; Komorowski, L. *Comp. Theor. Chem.* **2015,** *1065,* 42.
[37] Wang, G.; Xue, Y.; An, L.; Zheng, Y.; Dou, Y.; Zhang, L.; Liu, Y. *Food Chem.* **2015,** *171,* 89.
[38] Frisch, M. J.; Trucks, G. W.; Schlegel, H. B.; Scuseria, G. E.; Robb, M. A.; Cheeseman, J. R.; Montgomery Jr., J. A.; Vreven, T.; Kudin, K. N.; Burant, J. C.; Millam, J. M.; Iyengar, S. S.; Tomasi, J.; Barone, V.; Mennucci, B.; Cossi, M.; Scalmani, G.; Rega, N.; Petersson, G. A.; Nakatsuji, H.; Hada, M.; Ehara, M.; Toyota, K.; Fukuda, R.; Hasegawa, J.; Ishida, M.; Nakajima, T.; Honda, Y.; Kitao, O.; Nakai, H.; Klene, M.; Li, X.; Knox, J. E.; Hratchian, H. P.; Cross, J. B.; Adamo, C.; Jaramillo, J.; Gomperts, R.; Stratmann, R. E.; Yazyev, O.; Austin, A. J.; Cammi, R.; Pomelli, C.; Ochterski, J. W.; Ayala, P. Y.; Morokuma, K.; Voth, G. A.; Salvador, P.; Dannenberg, J. J.; Zakrzewski, V. G.; Dapprich, S.; Daniels, A. D.; Strain, M. C.; Farkas, O.; Malick, D. K.; Rabuck, A. D.; Raghavachari, K.; Foresman, J. B.; Ortiz, J. V.; Cui, Q.; Baboul, A. G.; Clifford, S.; Cioslowski, J.; Stefanov, B. B.; Liu, G.; Liashenko, A; Piskorz, P.; Komaromi, I.; Martin, R. L.; Fox, D. J.; Keith, T.; Al-Laham, M. A.; Peng, C. Y.; Nanayakkara, A.; Challacombe, M.; Gill, P. M. W.; Johnson, B.; Chen, W.; Wong, M. W.; Gonzalez, C.; Pople, J. A. *Gaussian 03. Revision B.01*. Gaussian Inc. Wallingford. CT. **2004**.
[39] Turker, L. *Propell. Explos. Pyrot.* **2015,** *40,* 180.
[40] Vosko, S. H.; Wilk, L.; Nusair, M. *Can. J. Phys.* **1980,** *58,* 1200.
[41] Lee, C.; Yang, W.; Parr, R. G. *Phys. Rev. B* **1988,** *37,* 785.
[42] Miehlich, B.; Savin, A.; Stoll, H.; Preuss, H. *Chem. Phys. Lett.* **1989,** *157,* 200.